Experimental Measurements of Regional Lung Deposition in Taiwanese

Chih-Wei Lin[1], Sheng-Hsiu Huang[1], Kuang-Nan Chang[1], Yu-Mei Kuo[2], Huey-Dong Wu[3], Chane-Yu Lai[4], Chih-Chieh Chen[1*]

[1]National Taiwan University, Taipei, Taiwan,
[2]Chung Hwa University of Medical Technology, Tainan, Taiwan,
[3]National Taiwan University Hospital, Taipei, Taiwan,
[4]Chung Shan Medical University, Taichung, Taiwan,

Abstract

Inhalation is the most important route of entry for aerosol particles. Aerosol deposition in the respiratory tract is affected by many factors, such as particle size, shape, charge, density, breathing pattern and the physical structure of the respiratory tract. However, currently available lung deposition data are mostly on Caucasians. Lung deposition data on Taiwanese are very limited. Therefore, it is essential to clarify whether there is a significant difference in respiratory tract deposition between Caucasians and Taiwanese. Thus, this work aimed to characterize regional lung deposition in Taiwanese.

A rapid regional lung deposition measurement method was employed in the present study. The experimental system consisted of an aerosol chamber, a mouthpiece, a pneumotachograph flow meter, and a particle counter. A cylinder-piston type breathing machine was used to generate a series of 'standard' breathing patterns for subjects to follow. In addition to mouth breathing, nose breathing was also conducted. A special respirator was employed to facilitate the measurements of nasal route deposition. The regional lung deposition data obtained in this work showed a good agreement with previous studies based on the bolus technique, indicating the difference in lung deposition between Taiwanese and Caucasians is negligible. The local deposition efficiency increased with penetration volume. This increased trend was particularly prominent in the deep lung, which was likely due to the dilution effect caused by the relatively clean air in the functional residual capacity. When a fixed fraction of forced vital capacity was used to replace

[*] Corresponding author. Tel: 886-2-33668086; Fax: 886-2-23938631
E-*mail address*: ccchen@ntu.edu.tw

fixed tidal volume, the total lung deposition became less dependent on the tidal volume. The nasal route local deposition efficiency was higher than that of the mouth route, but only in the early stage of penetration volume of 200 mL. This increase was mainly due to the nostril hairs and the complex configuration of the nasal turbinate.

Keywords: Aerosol deposition, Lung function, Breathing pattern, Tidal volume.

INTRODUCTION

Inhalation is the most important route for aerosol particles in the atmosphere to enter the body. The index of lung function measurement and the biological response caused by these inhaled particles vary with their site of deposition in the respiratory tract and the physiological or toxic effects within the target tissue. Particles in the ambient air are associated with adverse health effects such as cough, irritation, or allergy. The health effect can be acute or chronic. It depends on the particle composition, size, and the region of lung, so it is necessary to determine the total and regional distribution of particle deposition within the human respiratory tract for a proper evaluation of health risks. In addition, inhalation is an efficient way to deliver pharmaceutical aerosols used to treat respiratory diseases. Particles deposit within respiratory system depending on particles size distribution, shape, and charge condition (Ali et al., 2009; Cohen et al., 1998; Darquenne, 2012; Sturm and Hofmann, 2009). Further, it depends on breathing conditions such as breathing frequency, pause and flow rate (Inthavong et al., 2010; Kim and Hu, 2006; Kim and Jaques, 2005; Patterson et al., 2014).

Various methods have been applied to measure regional lung deposition. Previously, regional lung deposition has been measured by inhalation of particles labeled with g-emitting radionuclide (Hashish et al., 1998; Lippmann and Albert, 1969; Möller et al., 2006; Stahlhofen et al., 1980;

Rissler et al., 2017). However, subjects may be exposed to a high dosage of γ radionuclide. The process is quite cumbersome and time-consuming. Hollow models (cast) of human respiratory tract were frequently used to measure regional lung deposition (Ali et al., 2008; Chan and Lippmann, 1980; Grgic et al., 2006; Su and Cheng, 2006; Zhou et al., 2011). However, casts are not exactly the same as the real human respiratory tract, so making a realistic cast is still very challenging, especially for the peripheral parts of the lung. Recently, the serial bolus delivery method has been commonly employed to measured regional lung deposition (Brand et al., 1997; Heyder et al., 1988; Kim et al., 1996). The method is non-invasive, and does not require radioactive labelling of aerosols. However, measuring longitudinal distribution of deposited particles in the lungs using the bolus technique is still tedious and time-consuming and a high concentration of challenge aerosols is needed to ensure accurate measurement.

Until now, most experimental studies examining human regional lung deposition were on Caucasians. Lung deposition data on Taiwanese are very limited. Therefore, a database is needed to clarify whether there is a significant difference in respiratory tract deposition between Caucasians and Taiwanese. This is an essential step from the perspective of occupational hygiene, since it may profoundly affect the occupational hygiene regulations and standards. Therefore, this work aimed to characterize the regional lung deposition of Taiwanese.

METHODS

The experimental apparatus for rapid measurement of regional lung deposition is shown in Figure 1. To avoid hygroscopic growth of test aerosol in the respiratory tract, Di-2-ethylhexyl sebacate (DEHS) was chosen as the test agent. A condensation monodisperse aerosol generator (CMAG; Model 3475, TSI Inc., St. Paul, MN, U.S.A.) was chosen to generate micrometer-sized monodisperse DES aerosols. A constant output atomizer (Model 3075, TSI Inc.) and an electrostatic classifier (Model 3080, TSI Inc.) were used to generate submicrometer-sized monodisperse particles. Two aerosol size spectrometers were used to confirm the monodisperse size distribution and number concentration: an aerodynamic particle sizer (APS3321; TSI Inc.) for particles larger than 0.7 μm, and scanning mobility particle sizer (SMPS; Model 3936, TSI Inc.) for particles smaller than 0.6 μm. Before introducing the particles into the mixing chamber, a 25 mCi Am-241 radioactive source was used to neutralize the aerosol particles to the Boltzmann charge equilibrium. After the generated aerosols were introduced into the mixing chamber, a filtered dilution air flow of 100 L/min was employed to mix and carry the generated particles. A humidifier was employed to condition the filtered air to a relative humidity (RH) of 70-80 %. This was for the comfort of the human subjects.

97 The main sampling train used in a previous study (Chang et al., 2013) was slightly modified to
98 consist of a mouthpiece, a pneumotachograph flow meter (Fleisch 1TH), and a particle counter.
99 The mouthpiece was attached to the flow meter in line with a minimum dead space. In the present
100 study, a condensation particle counter (CPC; Model 3025, TSI Inc.) was used to measure the
101 particle number concentrations. During respiration, the aerosol was sampled continuously by
102 diverting a stream of air from the sampling train into the CPC via the sidearm port attached to the
103 mouthpiece. By using a PC-LabCard (PCI-1710HG-A, Advantech Inc., Taipei, Taiwan) and a
104 personal computer, the CPC measured the particle number concentration at a frequency of 100
105 Hz. All the air flows were controlled and monitored by mass flow controllers (Hasting
106 Instruments, Hampton, VA), which were calibrated against an electronic bubble meter (Gilibrator,
107 Gilian Instrument Crop., Wayne, NJ) or a wet gas meter if the flow was higher than 30 L/min.
108
109 A pressure transducer (PX653-01D5V, Omega Engineering Inc., Stamford, CT) and PC-
110 LabCard were connected to the flow meter to monitor the pressure change during breathing.
111 Before the test, a homemade cylinder-piston breathing machine (Cyclic flow model) was used to
112 generate a series of “standard” breathing patterns, i.e., combinations of different tidal volumes
113 and breathing frequencies. The subjects were instructed to practice and follow the breathing
114 pattern shown on a monitor. Standard breathing patterns were plotted on the computer monitor

115 placed in front of the subject for him/her to follow. It normally took subject more than 30 minutes
116 to learn to trace the breathing patterns.
117
118 There were 10 male and 2 female subjects recruited in the present study. All subjects were
119 asked to read and sign a consent form approved by the National Taiwan University. Subject
120 characteristics and lung function test results are shown in Table 1. The subjects could be
121 described as young and healthy. Each lung deposition test included at least 15 breathing cycles.
122 All tests were repeated at least 5 times a day and for more than 3 days. In addition to the fixed
123 tidal volume of 500 mL, the subjects were also asked to perform 20% of FVC (Forced Vital
124 Capacity) to examine the effect on lung deposition. A high fraction of FVC was not suitable to
125 perform because some subjects' high breathing flow might cause flow fluctuation of the particle
126 counter.
127
128 To estimate the longitudinal distribution of aerosol deposition, tidal volume can be divided into
129 infinitesimally small volume elements, or n elements. Aerosol particles within each volume
130 element of the respiratory tract system are assumed to have a regional deposition efficiency of xi
131 as they are inhaled and exhaled again with the same deposition efficiency penetrating through the

same volume element (i) (Kim et al., 1996; Brand et al., 1999). Aerosol recovery from the ith volume element, RCi, can be obtained by

$$RC_i = \prod_{k=1}^{i} (1 - x_k)^2 \quad (1)$$

Aerosol deposition fraction in ith volume element (DFi) is the sum of depositions during inspiration and expiration. The local deposition fraction in the ith volume element, LDFi, can then be expressed as

$$LDF_i = \frac{1}{n} \sum_{j=1}^{n} DF_i \quad (2)$$

In addition to mouth breathing, nose breathing was also performed in the present study. A special respirator was employed to facilitate the nasal route deposition experiments. The space of a nose respirator together with the sample train was about 50 cm3, almost the same as the mouth route. Before nose breathing tests, the leakage test was performed to ensure the special respirator was well fitted for the subject.

RESULTS AND DISCUSSION

Twelve subjects completed lung deposition efficiency measurements for the 1 μm particle at a tidal volume of 500 mL and breathing frequency of 15 bpm. Figure 2 shows the local deposition

efficiency curves for each 50-mL volumetric region as a function of penetration volume for all 12 subjects. The trend (circle symbol with solid line) of Taiwanese regional lung deposition was similar to Kim's data (Kim et. al., 1996), showing that local deposition values increased with increasing penetration volume. However, the local deposition efficiency (0-400 mL) measured in the present study was slightly higher (about 1~3 %) than Kim's. Yet, the difference in local deposition efficiency increased sharply when entering the deep penetration volume (400-500 mL). This mismatch with Kim's data was likely due to (1) the two experimental systems not being exactly the same: the bolus technique was used in Kim's study, while the rapid measurement system was employed in the present study; and (2) the breathing patterns differed: constant velocity was adopted in Kim's study, while the sinusoidal patterns was used in this work. Further, the difference in the deep lung was likely due to the dilution effect caused by the clean air staying in the functional residual capacity (FRC). Note, aerosol particles remaining in the FRC were very likely deposited due to either diffusion (for small particles) or gravitational settling (for large particles) because of long retention time. Therefore, the FRC air could be regarded as aerosol-free to dilute the aerosol concentration entering the alveolar region.

Moreover, the regional lung deposition of each subject might vary quite significantly, as shown in Figure 3. For example, subject 7 had higher regional lung deposition than subject 5 throughout

all penetration volume. These two subjects began to show different regional deposition efficiency values after the first 50 mL, or the mouth region. This mismatch was particularly pronounced in the 300 mL of volumetric lung region, and the difference slightly shrank if going further into the alveolar region. Both subjects were asked to perform the same breathing pattern of tidal volume 500 mL and breathing frequency of 15 breaths/min. Since both subjects shared about the same lung function and deposition efficiency curves were very repeatable, the difference in regional lung deposition was likely due to anatomical and physiological reasons, i.e. the dimensions of the respiratory tract and/or the thickness of the mucus layer.

The local deposition efficiency values of subject 1 over 15 months are shown in Figure 4. The data were repeated at least 3 times each month. The results indicated the trend of local deposition efficiency was consistent and always increased with increasing penetration volume. However, the local deposition efficiency values might vary with time but not in a particular order. The difference between the highest and lowest deposition efficiency curves was about a factor of 2. The reasons for this inconsistency require further investigation.

The regional lung deposition efficiency data could be integrated to form total lung deposition efficiency data. In the present study, the total lung deposition for particles sizing from 20 nm to 1

μm, at tidal volume 500 mL and breathing frequency 15 bpm were shown in Figure 5, to compare with Kim's (Jaques and Kim, 2000; Kim and Hu, 2006) and Heyder's data (Heyder et al., 1986). Both male and female data of Kim agreed quite well with the solid line which was the best-fit of Heyder's data. In Figure 5, the total deposition fraction decreased with increasing particle size from 20 to 300 nm, apparently because of decreasing particle diffusivity. For particles larger than 300 nm, the total deposition fraction then increased with increasing particle size because of increasing inertial impaction. Overall, the deposition efficiency curve showed a "collection minimum" at 0.3 μm, an apparent characteristic of the mechanical filter. The deposition efficiency data collected in this work showed good agreement with previous studies, and although our data were slightly lower, the difference was not statistically significant.

In general, the data analysis of regional lung deposition in previous studies was all based on fixed tidal volume. However, lung function varied among voluntary subjects, as shown in Table 1. For example, the forced vital capacity ranged from 2.91 L (subject 11) to 4.79 L (subject 10), indicating people breathed differently in terms of tidal volume. Therefore, it was of interest to measure the lung deposition at 20% FVC, in addition to the fixed tidal volume of 500 mL. Figure 6 shows the total deposition of both fixed tidal volume of 500 mL and 20% FVC of 7 subjects, breathing 1 μm particle at 15 bpm. For fixed tidal volume, the deposition fraction varied, ranging

from 0.13 to 0.18. The deposition fraction of each subject was higher when performing 20% FVC, because the minute volume was higher than 500 mL. Lung deposition increasing with increasing tidal volume under the same breathing frequency has been well documented, because the aerosol particles had to travel a greater distance into the deep lung, resulting in higher aerosol deposition. However, the deposition efficiency of 20% FVC was clearly less dependent on tidal volume, indicating aerosol deposition efficiency was about the same for participating subjects. Nevertheless, the deposited aerosol mass increased with increasing tidal volume. A higher fraction than 20% FVC was not conducted because, for some subjects, the breathing flows were too high, which caused fluctuation in the sampling flow of CPC.

Lung deposition measurements were normally conducted through the mouth route, but not the nose. This was because of less aerosol deposition in the mouth and more consistent anatomical dimensions of the mouth-laryngeal channel. On the other hand, the variations in nostril hairs, mucus layer in the nasal cavity, and the face-seal of the respirator, all made the nasal route measurements more challenging. In Figure 7, both local deposition efficiency curves (monodisperse 1 μm aerosol particles and breathing frequency of 15 bpm) through the mouth and nose were shown and compared. The nasal route showed higher deposition efficiency in the early stage of penetration volume of 200 mL, likely due to the complex configuration of the nasal

turbinate. The deposition efficiency curves downstream of the trachea (after 200 mL) were almost identical. This is because the same subject performed the same breathing maneuver, almost at the same time.

CONCLUSIONS

The regional lung deposition data obtained using the newly developed rapid measurement system, showed good agreement with previous studies based on the bolus technique. The difference in total lung deposition between Taiwanese and Caucasians was found to be negligible. The total lung deposition curve as a function of particle size showed deposition efficiency of particles smaller than 0.3 μm increased with decreasing particle size, while the deposition efficiency of particles larger than 0.3 μm increased with increasing particle size. This is because small particles tend to be collected by diffusion; while large particles tend to be collected due to inertial impaction. The collection minimum appeared at around 0.3 μm, indicating the human lung had the same filtration characteristics as a mechanical filter.

The local deposition efficiency of Taiwanese was higher than that in Kim's study. This difference might be due to (1) different measurement systems being employed: rapid measurement system in this work, but the bolus technique in the previous study, and (2) different breathing patterns were used: sinusoidal wave in the present study and constant flow in previous

241 studies. The difference in local deposition efficiency was especially noticeable in the deep lung
242 region (400-500 mL). We speculated this phenomenon was due to the dilution effect caused by
243 the relatively clean air in the functional residual capacity. More studies are needed to validate this
244 phenomenon of FRC dilution.
245
246 The trend of local deposition efficiency in each subject was quite consistent, but varied with
247 time. The between-subject variation was significant, even for subjects with about the same lung
248 function. For each participating subject, total deposition fraction increased with increasing tidal
249 volume, because aerosol particles had to travel a greater distance and flow through more surface
250 area. However, the total deposition varied even with fixed tidal volume, because the lung
251 functions of test subjects differed. Further, when a fixed fraction of FVC was employed to
252 replace fixed tidal volume, the total deposition fraction became less dependent on the tidal
253 volume, indicating the deposition efficiency during normal breathing is about the same for all
254 subjects. Nevertheless, a person with higher tidal volume collects a greater amount of aerosol
255 deposit.
256
257 The nasal route local deposition efficiency was higher than that of the mouth route, but only in
258 the early stage of penetration volume of 200 mL. The deposition efficiency curves downstream of

the trachea (after 200 mL) were almost identical for both nose- and mouth-breathing. This mismatch was mainly due to the nostril hairs and the complex configuration in the nasal turbinate region, resulting in higher aerosol deposition.

ACKNOWLEDGMENTS

The authors would like to thank the Ministry of Science and Technology of Taiwan (Grant No. MOST 105-3011-F-002-008) for the financial supports.

REFERENCES

Ali, M., Mazumder, M. K. and Martonen, T. B. (2009). Measurements of Electrodynamic Effects on the Deposition of Mdi and Dpi Aerosols in a Replica Cast of Human Oral-Pharyngeal-Laryngeal Airways. J. Aerosol Med. Pulm. Drug Deliv. 22:35-44.

Ali, M., Reddy, R. N. and Mazumder, M. K. (2008). Electrostatic Charge Effect on Respirable Aerosol Particle Deposition in a Cadaver Based Throat Cast Replica. J. Electrostatics 66:401-406.

Brand, P., Rieger, C., Schulz, H., Beinert, T. and Heyder, J. (1997). Aerosol Bolus Dispersion in Healthy Subjects. Eur. Respir. J. 10:460-467.

Chang, K.N., Huang, S.H., Chen, C.W., Wu, H.D., Chen, Y.K., Lai, C.Y., Chen, C.C. (2013). A

279 Sampling Train for Rapid Measurement of Regional Lung Deposition. Aerosol and Air Quality
280 Research, 13: 608–617.

281 Chan, T. L. and Lippmann, M. (1980). Experimental Measurements and Empirical Modelling of
282 the Regional Deposition of Inhaled Particles in Humans. Am. Ind. Hyg. Assoc. J. 41:399-409.

283 Cohen, B. S., Xiong, J. Q., Fang, C. P. and Li, W. (1998). Deposition of Charged Particles on
284 Lung Airways. Health Phys. 74:554-560.

285 Darquenne, C. (2012). Aerosol Deposition in Health and Disease. J. Aerosol Med. Pulm. Drug
286 Deliv. 25:140-147.

287 Grgic, B., Martin, A. R. and Finlay, W. H. (2006). The Effect of Unsteady Flow Rate Increase on
288 in Vitro Mouth-Throat Deposition of Inhaled Boluses. J. Aerosol Sci. 37:1222-1233.

289 Hashish, A. H., Fleming, J. S., Conway, J., Halson, P., Moore, E., Williams, T. J., Bailey, A. G.,
290 Nassim, M. and Holgate, S. T. (1998). Lung Deposition of Particles by Airway Generation in
291 Healthy Subjects: Three-Dimensional Radionuclide Imaging and Numerical Model Prediction.
292 J. Aerosol Sci. 29:205-215.

293 Heyder, J., Blanchard, J. D., Feldman, H. A. and Brain, J. D. (1988). Convective Mixing in
294 Human Respiratory Tract: Estimates with Aerosol Boli. J. Appl. Physiol. 64:1273-1278.

295 Heyder, J., Gebhart, J., Rudolf, G., Schiller, C. F. and Stahlhofen, W. (1986). Deposition of

296 Particles in the Human Respiratory Tract in the Size Range 0.005-15 Mm. J. Aerosol Sci.
297 17:811-825.

298 Inthavong, K., Choi, L.-T., Tu, J., Ding, S. and Thien, F. (2010). Micron Particle Deposition in a
299 Tracheobronchial Airway Model under Different Breathing Conditions. Medical Engineering
300 & Physics 32:1198-1212.

301 Jaques, P. A. and Kim, C. S. (2000). Measurement of Total Lung Deposition of Inhaled Ultrafine
302 Particles in Healthy Men and Women. Inhal. Toxicol. 12:715-731.

303 Kim, C. S. and Hu, S. C. (2006). Total Respiratory Tract Deposition of Fine Micrometer-Sized
304 Particles in Healthy Adults: Empirical Equations for Sex and Breathing Pattern. J. Appl.
305 Physiol. 101:401-412.

306 Kim, C. S., Hu, S. C., DeWitt, P. and Gerrity, T. R. (1996). Assessment of Regional Deposition
307 of Inhaled Particles in Human Lungs by Serial Bolus Delivery Method. J. Appl. Physiol.
308 81:2203-2213.

309 Kim, C. S. and Jaques, P. A. (2005). Total Lung Deposition of Ultrafine Particles in Elderly
310 Subjects During Controlled Breathing. Inhal. Toxicol. 17:387-399.

311 Lippmann, M. and Albert, R. E. (1969). The Effect of Particle Size on the Regional Deposition of
312 Inhaled Aerosols in the Human Respiratory Tract. Am. Ind. Hyg. Assoc. J. 30:257-275.

313 Möller, W., Felten, K., Seitz, J. g., Sommerer, K., Takenaka, S., Wiebert, P., Philipson, K.,
314 Svartengren, M. and Kreyling, W. G. (2006). A Generator for the Production of Radiolabelled
315 Ultrafine Carbonaceous Particles for Deposition and Clearance Studies in the Respiratory Tract.
316 J. Aerosol Sci. 37:631-644.

317 Patterson, R.F., Zhang, Q., Zheng, M., Zhu, Y. (2014). Particle Deposition in Respiratory Tracts
318 of School-Aged Children. Aerosol and Air Quality Research, 14: 64–73.

319 Rissler, J., Nicklasson, H., Gudmundsson, A., Wollmer, P., Swietlicki, E., Löndahl, J. (2017). A
320 Set-up for Respiratory Tract Deposition Efficiency Measurements (15–5000 nm) and First
321 Results for a Group of Children and Adults. Aerosol and Air Quality Research, 17: 1244–1255.

322 Stahlhofen, W., Gebhart, J. and Heyder, J. (1980). Experimental Determination of the Regional
323 Deposition of Aerosol Particles in the Human Respiratory Tract. Am. Ind. Hyg. Assoc. J.
324 41:385-398a.

325 Sturm, R. and Hofmann, W. (2009). A Theoretical Approach to the Deposition and Clearance of
326 Fibers with Variable Size in the Human Respiratory Tract. J. Hazard. Mater. 170:210-218.

327 Su, W.-C. and Cheng, Y. S. (2006). Deposition of Fiber in a Human Airway Replica. J. Aerosol
328 Sci. 37:1429-1441.

329 Zhou, Y., Sun, J. and Cheng, Y. S. (2011). Comparison of Deposition in the Usp and Physical

330 Mouth-Throat Models with Solid and Liquid Particles. J Aerosol Med Pulm Drug Deliv
331 24:277-284.

332

333

334

335

Table 1. Subject characteristics and lung function test results

Subject	Gender	Age	Height, cm	Weight, Kg	FVC, L	FEV1, L	VT, L	20% FVC, L
1	M	29	160	62	3.37	2.79	0.65	0.67
2	M	24	171	84	5.18	4.67	0.55	1.04
3	F	23	158	48	3.11	2.74	0.45	0.62
4	M	37	168	60	4.14	4.04	0.75	0.83
5	M	23	172	60	4.6	3.72	0.73	0.92
6	M	29	174	79	3.43	2.9	0.72	0.67
7	M	33	175	68	4.64	3.95	0.82	0.93
8	M	25	170	69	4.09	3.45	0.63	0.82
9	M	24	170	60	4.27	3.84	0.64	0.85
10	M	22	180	65	4.79	4.09	0.6	0.96
11	F	22	156	50	2.91	2.47	0.67	0.58
12	M	22	175	60	4.61	3.88	0.61	0.92

FVC, forced vital capacity; FEV1, forced expiratory volume in 1 s; VT, Tidal Volume

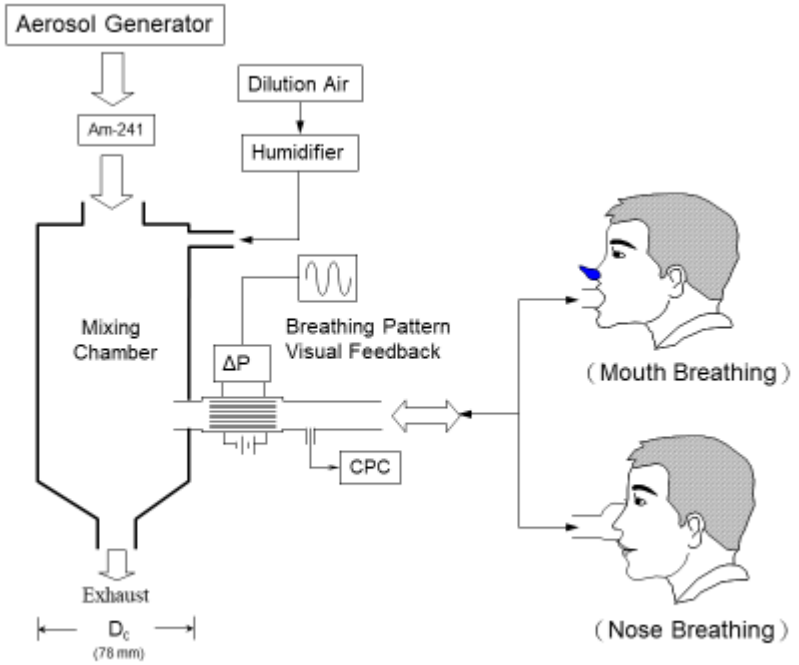

Figure 1. Schematic diagram of the experimental system set-up.

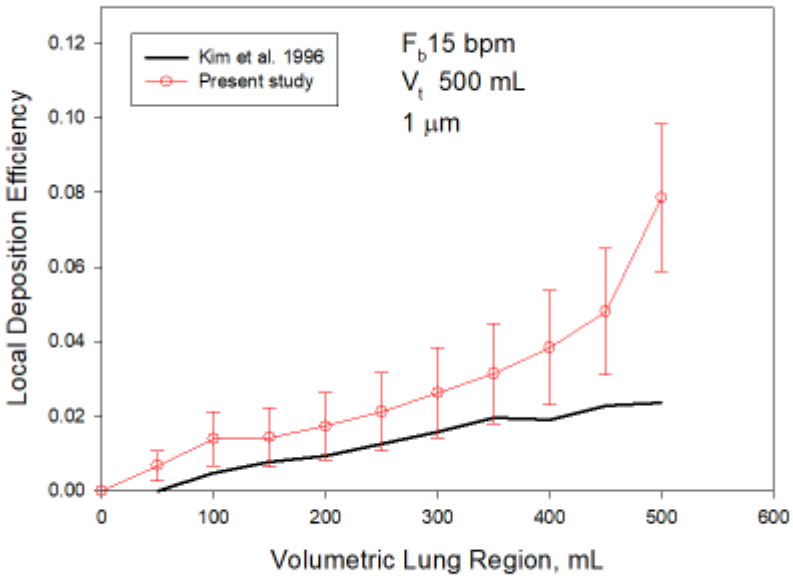

Figure 2. Local deposition efficiency (for each 50 ml volumetric region) as a function of penetration volume compared with Kim's data

340

341

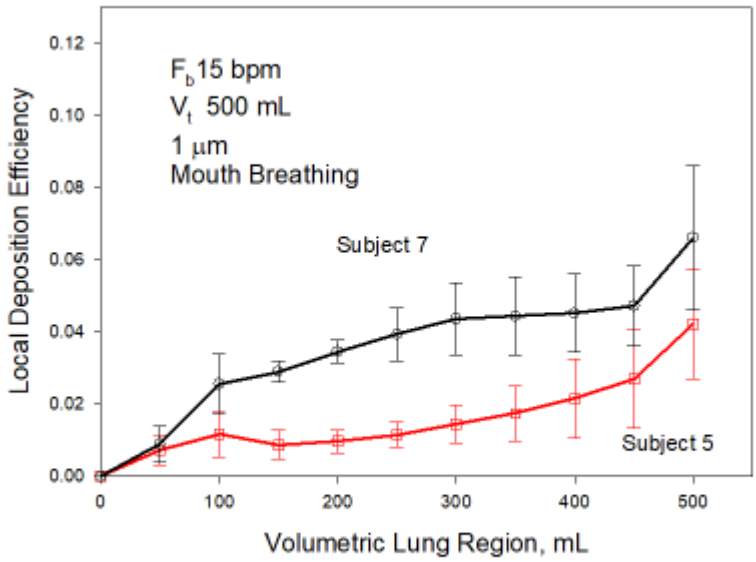

Figure 3. Comparison of local deposition efficiency of subject 5 and 7 for mouth breathing

342

343

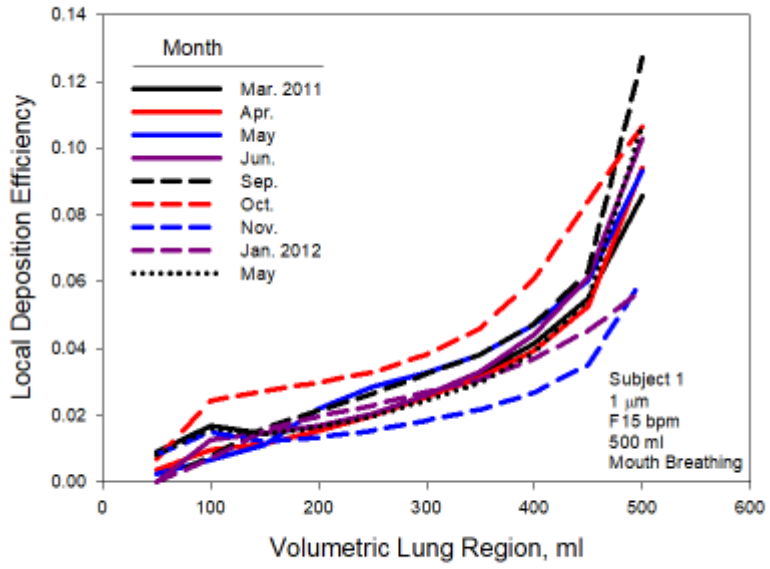

344 Figure 4. Local deposition efficiency of subject 1 in different months

345

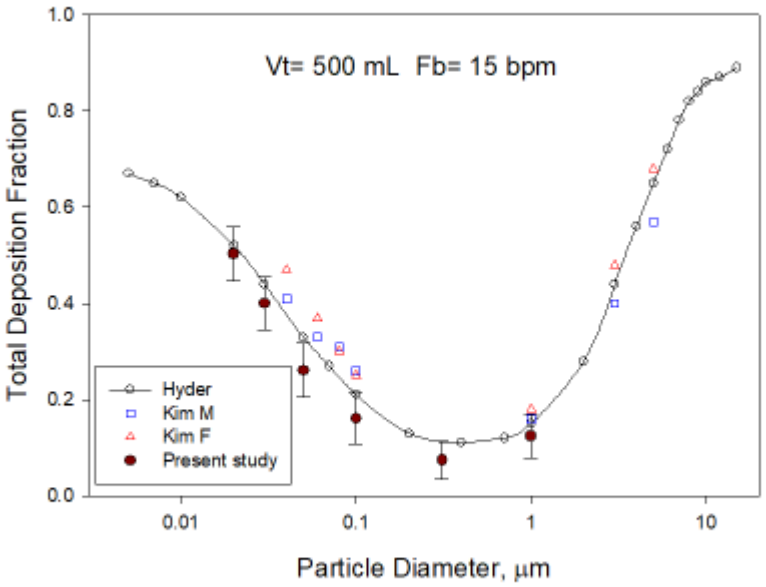

346 Figure 5. Total deposition Fraction compared with Kim's & Hyder's data

347

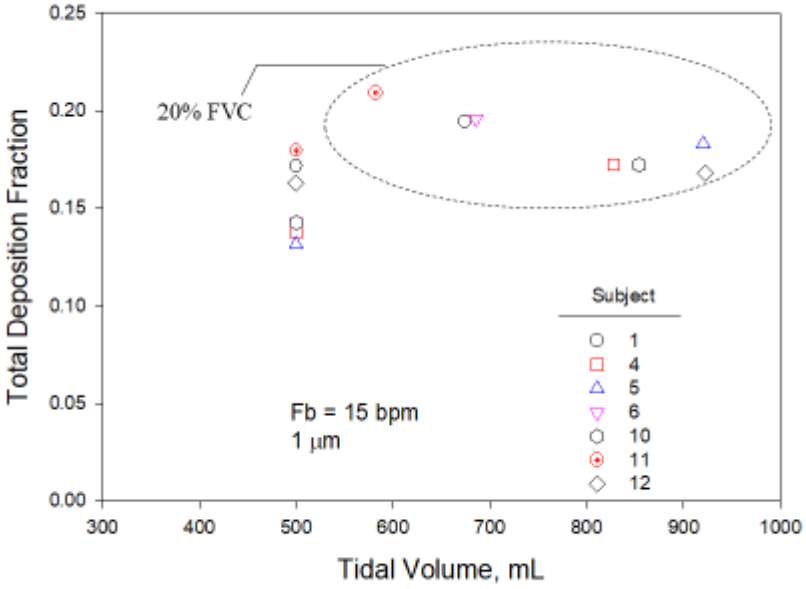

Figure 6. Comparison of total deposition fraction at fix 500 mL and 20% FVC as tidal volume

348

349

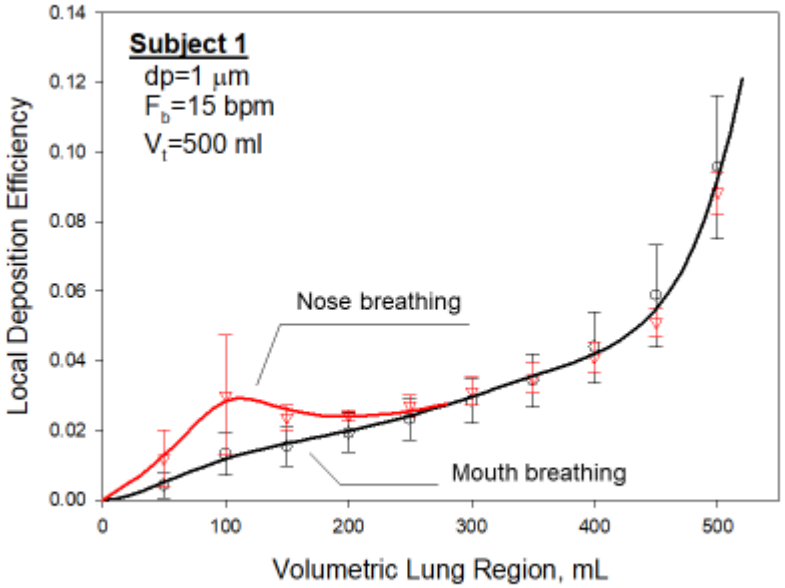

Figure 7. Comparison of local deposition efficiency measured by nose and mouth breathing

350

351

352

353 **Table Captions**

354 Table 1. Subject characteristics and lung function test results

355

356 **Figure Captions**

357 Fig. 1. Schematic diagram of the experimental system set-up.

358 Fig. 2. Local deposition efficiency (for each 50 ml volumetric region) as a function of penetration

359 volume compared with Kim's data.

360 Fig. 3. Comparison of local deposition efficiency of subject 5 and 7 for mouth breathing.

361 Fig. 4. Local deposition efficiency of subject 1 in different months.

362 Fig. 5. Total deposition Fraction compared with Kim's & Hyder's data

363 Fig. 6. Comparison of total deposition fraction at fix 500 mL and 20% FVC as tidal volume

364 Fig. 7. Comparison of local deposition efficiency measured by nose and mouth breathing

365